Available online at www.sciencedirect.com
SCIENCE DIRECT
International Journal of Heat and Mass Transfer 49 (2006) 1129–1136
International Journal of HEAT and MASS TRANSFER
www.elsevier.com/locate/ijhmt

Asymptotic analysis of heat transfer in turbulent Rayleigh–Bénard convection

M. Hölling *, H. Herwig

Hamburg University of Technology, Applied Thermodynamics, Denickestraße 17, D-21073 Hamburg, Germany

Received 18 April 2005; received in revised form 21 July 2005
Available online 27 October 2005

Abstract

Based on asymptotic considerations a heat transfer law for turbulent Rayleigh–Bénard convection is found that differs from existing correlations which often are of a power law type with respect to their Rayleigh number dependence. From the asymptotic temperature profile, derived by matching temperature gradients in the overlap region of the wall layer and the core layer, a Nusselt number follows which includes a logarithmic term. This correlation is in good agreement with data from highly accurate Rayleigh–Bénard experiments for Rayleigh numbers between 10^5 and 10^{15} and Prandtl numbers larger than 0.5. It is an alternative to existing power laws or more complicated correlations for $Nu = Nu(Ra,Pr)$.

1. Introduction

In Rayleigh–Bénard convection flows a fluid is confined between two parallel horizontal plates, a hot bottom plate and a cold top plate. Once a critical value of the characteristic parameters is reached the fluid starts moving due to density differences and heat is transferred mainly by convection. The Nusselt number $Nu \equiv |\partial T/\partial y|_w \cdot h/\Delta T$ then only depends on the Rayleigh number $Ra = g\beta\Delta T h^3/(\nu a)$, the Prandtl number $Pr = \nu/a$ and the geometry characterised by the aspect ratio $\Gamma = d/h$.

Though the geometry is simple and intensive experimental and theoretical investigations have been performed in the last decades there is still a controversy whether a simple power law for $Nu = Nu(Ra,Pr,\Gamma)$ is adequate.

For a long time it was accepted that for high Rayleigh numbers the heat flux is independent of the plate distance h. This implies to $Nu \sim Ra^{1/3}$ since $Nu \sim h$ and $Ra \sim h^3$, see Priestley [1].

Castaing et al. [2] performed experiments over a wide range of Rayleigh numbers with improved accuracy compared to earlier studies and found $Nu = 0.23 \cdot Ra^{0.282}$ for $Pr \approx 1$. They developed a new theory with an exponent $2/7 = 0.286$ for Ra quite close to their experimentally found value. Shraiman and Siggia [3] provided an alternative derivation of the 2/7th power law based on boundary layer considerations. Wu and Libchaber [4] experimentally determined $Nu = 0.146 \cdot Ra^{0.286}$ and Kerr [5] numerically found $Nu = 0.186 \cdot Ra^{0.276}$, all in favour of the 2/7-law which thus seemed to be established.

In a more sophisticated approach Grossmann and Lohse [6] developed a theory based on the kinematic and thermal dissipation rates in the bulk and the boundary layer. They identified different regimes with individual scalings and obtained $Nu(Ra,Pr)$ by a superposition of the scaling laws in neighbouring regimes. Xu et al. [7], for example, found good agreement between their measurements and this theory. For an extension to large Prandtl numbers, see [8].

Niemela et al. [9] in their experiments covered a wide range of Rayleigh numbers ($10^6 \leqslant Ra \leqslant 10^{17}$) and for $Pr \approx 1$ found $Nu = 0.124 \cdot Ra^{0.309}$ which is between the 1/3 and 2/7-laws but cannot be interpreted properly by

* Corresponding author. Tel.: +49 40 42878 3497; fax: +49 40 42878 2967.
E-mail addresses: m.hoelling@tu-harburg.de (M. Hölling), h.herwig@tu-harburg.de (H. Herwig).

0017-9310/$ - see front matter © 2005 Elsevier Ltd. All rights reserved.
doi:10.1016/j.ijheatmasstransfer.2005.09.002

Nomenclature

a	molecular thermal diffusivity
d	width of experimental setup
C	constant of temperature profile
D	parameter of temperature profile
g	gravitational acceleration
h	vertical distance between the two plates
k_s	surface roughness
$k_{s\,eq}$	equivalent sand roughness
$k_s^\times$	non-dimensionalized surface roughness, $k_s/T_c \cdot \lvert\partial T/\partial y\rvert_w$
Ra	Rayleigh number, $g\beta\Delta T h/(va)$
Nu	Nusselt number, $h/\Delta T \cdot \lvert\partial T/\partial y\rvert_w$
Pr	Prandtl number, v/a
T	mean temperature
$\lvert\partial T/\partial y\rvert_w$	absolute value of temperature gradient at the wall
T_c	characteristic temperature, $[av\lvert\partial T/\partial y\rvert_w^3/(g\beta)]^{1/4}$
T_{cold}	temperature of cold wall
T_h	temperature of hot wall
ΔT	temperature difference between top and bottom plate
$\bar{u}$	mean horizontal velocity component
$\bar{v}$	mean vertical velocity component
$-\overline{v'T'}$	turbulent heat flux
x	coordinate parallel to the wall
y	coordinate normal to the wall
$y^\times$	non-dimensionalized wall distance, $y/T_c \cdot \lvert\partial T/\partial y\rvert_w$
$\hat{y}$	intermediate variable, $y/(h^{(1-\alpha)}\delta^\alpha)$

Greek symbols

α	exponent in the intermediate variable $\hat{y}$, $0 \leqslant \alpha \leqslant 1$
β	coefficient of thermal expansion
δ	scale for the height of the wall layer, $T_c/\lvert\partial T/\partial y\rvert_w$
η	non-dimensionalized wall distance in the core layer, y/h
Γ	aspect ratio, d/h
v	molecular kinematic viscosity
$\Theta^\times$	non-dimensionalized temperature, $(T_h - T)/T_c$

existing theories. They also mentioned that the choice of fluid properties is an important aspect in correlating data. They reconsidered the data of Wu and Libchaber [4] with fluid properties of improved accuracy and obtained $Nu \sim Ra^{0.299}$ instead of $Nu \sim Ra^{0.286}$.

Ahlers [10] and Verzicco [11] examined the influence of sidewall conduction and found that it cannot be neglected or corrected by the heat transfer rates in evacuated experimental set-ups. Ahlers [10] proposed a correction to account for the heat flux in different wall materials and, for example, recalculated the data of Niemela et al. [9] getting $Nu \sim Ra^{0.318}$ instead of $Nu \sim Ra^{0.309}$. These studies show that experimental data have to be analysed very carefully.

In recent experiments, for example by Ashkenazi and Steinberg [12], Chavanne et al. [13], Nikolaenko and Ahlers [14], Niemela and Sreenivasan [15] and Roche et al. [16], the effect of sidewall conduction could either be neglected due to a modified experimental set-up or was corrected by an analytical approach. These data as well as numerical data, where heat conduction in walls is absent, are taken as reference data in Section 3 of our study.

Different from previous theoretical studies, we first derive an expression for the temperature profile. This is done in Section 2 by asymptotic matching of gradients like for forced and natural convection flow fields, see Schlichting and Gersten [17], Hölling and Herwig [18], respectively. Once the temperature profile can be descriped properly, a Nusselt number correlation can be deduced (Section 3) leading to a new Nusselt number correlation based on asymptotic considerations, i.e. being asymptotically correct for $Ra \to \infty$.

2. Temperature profile

We consider a Rayleigh–Bénard flow with plates of infinite extent as studied numerically by Kerr [5], Grötzbach [19], Wörner [20][1] and Hartlep [21] for $Pr = 0.71$. Due to the infinite extension of the plates, there is no time-averaged local mean flow (i.e. $\bar{u} = \bar{v} = 0$). Thus, only an expression for the temperature profile has to be found.

With no mean flow and plates of infinite extent (i.e. with no gradients in x-direction, $\partial(\cdots)/\partial x = 0$) the energy equation is reduced to

$$0 = \frac{\partial}{\partial y}\left[a\frac{\partial T}{\partial y} - \overline{v'T'}\right] \Rightarrow a\left.\frac{\partial T}{\partial y}\right|_w = a\frac{\partial T}{\partial y} - \overline{v'T'}. \tag{1}$$

Obviously, $a \cdot \partial T/\partial y|_w$ is a characteristic quantity of the Rayleigh–Bénard convection since $a \cdot \partial T/\partial y - \overline{v'T'}$, which is basically the total heat flux, is constant for all $0 \leqslant y \leqslant h$ and equal to $a \cdot \partial T/\partial y|_w$. Therefore, a characteristic reference temperature can be defined with the temperature gradient at the wall, i.e.

$$T_c \equiv \left(\frac{av}{g\beta}\left|\frac{\partial T}{\partial y}\right|_w^3\right)^{1/4}. \tag{2}$$

[1] The data of [19] and [20] are available at the homepage of the institute for reactor safety (research center Karlsruhe): http://hikwww4.fzk.de/irs/irs3/.

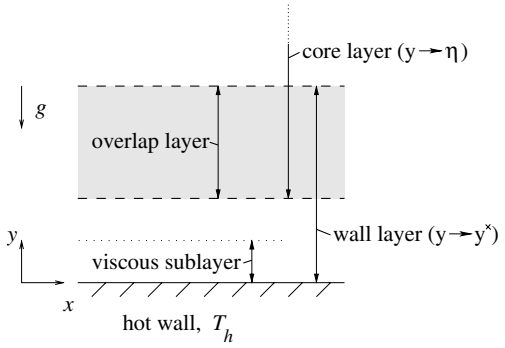

Fig. 1. Two-layer structure near the hot wall. Adjacent to the wall exists a sublayer with only molecular heat flux as a part of the wall layer. The wall layer has no sharp edge towards the core layer, instead an overlap layer exists in between. Wall layer and core layer variables are valid simultaneously in the overlap layer.

A similar characteristic temperature holds for natural convection on vertical walls, see Hölling and Herwig [18]. Here, T_c according to Eq. (2) is used to non-dimensionalize the temperature difference, which without loss of generality can be defined at the hot plate temperature:

$$\Theta^{\times} \equiv \frac{T_h - T}{T_c} \tag{3}$$

For $Ra \to \infty$ the flow-field has a two-layer-structure, with a region close to the wall where molecular and turbulent heat flux are present (wall layer) and the bulk with only turbulent heat flux (core layer), see Fig. 1. An appropriate scale for the wall layer thickness is

$$\delta \equiv \frac{T_c}{|\partial T/\partial y|_w} \tag{4}$$

with

$$\lim_{Ra\to\infty} \frac{\delta}{h} = 0 \tag{5}$$

thus leading to a singularity at the wall.[2] A non-dimensional wall distance in the wall layer that does not degenerate is

$$y^{\times} \equiv \frac{y}{\delta} = \left|\frac{\partial T}{\partial y}\right|_w \cdot \frac{y}{T_c} \tag{6}$$

since for all values of y within the wall layer $\lim_{Ra\to\infty}(y/\delta) = O(1)$.

The wall distance in the core layer, non-dimensionalized with h, is $\eta \equiv y/h$. Here, $y^{\times}$ would be inappropriate since, for example, at $y = h/2$

$$\lim_{Ra\to\infty} \left(\left|\frac{\partial T}{\partial y}\right|_w \cdot \frac{h/2}{T_c}\right) \to \infty. \tag{7}$$

The wall layer and the core layer asymptotically overlap and thus can be described in both variables (i.e. $y^{\times}$ and η) in this overlap layer. The temperature profile is obtained by matching the gradients in this overlap region where an intermediate variable $\hat{y} = y/(h^{1-\alpha}\delta^{\alpha})$ with $0 \leqslant \alpha \leqslant 1$ exists, so that $\eta \leqslant \hat{y} \leqslant y^{\times}$, see for example Schlichting and Gersten [17]. Temperature gradients, approaching the overlap layer from both sides, should be the same $\partial\Theta^{\times}/\partial\hat{y}$, i.e.

$$\frac{\partial\Theta^{\times}}{\partial\hat{y}} = \lim_{y^{\times}\to\infty} \frac{\partial\Theta^{\times}(y^{\times})}{\partial y^{\times}} \frac{\partial y^{\times}}{\partial\hat{y}} = \lim_{y^{\times}\to\infty} \frac{h^{1-\alpha}\delta^{\alpha}}{\delta} \cdot \frac{\partial\Theta^{\times}(y^{\times})}{\partial y^{\times}} \tag{8}$$

$$\frac{\partial\Theta^{\times}}{\partial\hat{y}} = \lim_{\eta\to 0} \frac{\partial\Theta^{\times}(\eta)}{\partial\eta} \frac{\partial\eta}{\partial\hat{y}} = \lim_{\eta\to 0} \frac{h^{1-\alpha}\delta^{\alpha}}{h} \cdot \frac{\partial\Theta^{\times}(\eta)}{\partial\eta}. \tag{9}$$

Equating (8) and (9) leads to

$$\lim_{y^{\times}\to\infty} y^{\times} \frac{\partial\Theta^{\times}(y^{\times})}{\partial y^{\times}} = \lim_{\eta\to 0} \eta \frac{\partial\Theta^{\times}(\eta)}{\partial\eta} \tag{10}$$

after both sides have been multiplied by y. In general, Eq. (10) can only be fulfilled if both sides are the same constant C. Therefore

$$\lim_{y^{\times}\to\infty} \frac{\partial\Theta^{\times}(y^{\times})}{\partial y^{\times}} = \frac{C}{y^{\times}} \tag{11}$$

which, after an integration over the wall layer, leads to

$$\lim_{y^{\times}\to\infty} \Theta^{\times} = C\ln(y^{\times}) + D. \tag{12}$$

This is the asymptotic temperature profile which holds close to but not at the wall.

2.1. Viscous sublayer

For the region adjacent to the wall the temperature profile can be derived as following. Here, turbulent fluctuations are completely damped by the wall ($\overline{v'T'} = 0$) and a purely molecular sublayer exists as part of the wall layer. Integrating the energy equation $\partial^2 T/\partial y^2 = 0$ we get for the temperature profile

$$T_h - T = \left|\frac{\partial T}{\partial y}\right|_w \cdot y \tag{13}$$

or in its non-dimensional form

$$\frac{T_h - T}{T_c} = \left|\frac{\partial T}{\partial y}\right|_w \cdot \frac{y}{T_c} \Rightarrow \Theta^{\times} = y^{\times}. \tag{14}$$

2.2. Comparison with experimental and numerical data

Measured and calculated (DNS) data can be used to check the general form (12) for $\Theta^{\times}$ and to determine its constants C and D. Unfortunately, only very few detailed temperature profiles are available though numerous experiments have been performed in order to determine Nusselt numbers. There also is only a limited range of Rayleigh numbers for which experimental and DNS data can be found, see Chavanne et al. [13] for an overview.

In Table 1 the sources for the temperature profiles are listed which we used to validate our asymptotic temperature profile (12).

[2] $T(y=0) = T_h$, but $\lim_{\delta\to 0} T(y=\delta) = T_h - \Delta T/2$, with T_h being the temperature of the hot wall at $y = 0$ and $\Delta T = T_h - T_{cold}$.

Table 1
Sources for DNS data and measured temperature profiles compared to Eq. (12) in order to determine C and D

Reference	Ra	Pr	Type	Nu
Kerr [5]	2×10^7	0.7	DNS	$0.186\cdot Ra^{0.276}$
Grötzbach [19]	3.81×10^5	0.7	DNS	–
Wörner [20]	6.3×10^5	0.7	DNS	–
Hartlep [21]	10^6, 10^7	0.7	DNS	$0.175\cdot Ra^{0.278}$
Du [22]	1.5×10^9	5.4	exp.	$0.17\cdot Ra^{0.29}$
Chu [23]	$9.34\times10^6 \div 1.86\times10^7$	5.4	exp.	$0.183\cdot Ra^{0.278}$

The data sets of Table 1 are plotted in their non-dimensionalized form, i.e. $\Theta^\times$ and $y^\times$, in Fig. 2 (DNS data) and in Fig. 3 (experimental data). All data sets can be fitted to a logarithmic profile with a constant slope $C = 0.1$. The value of D, however, depends on the Rayleigh number.

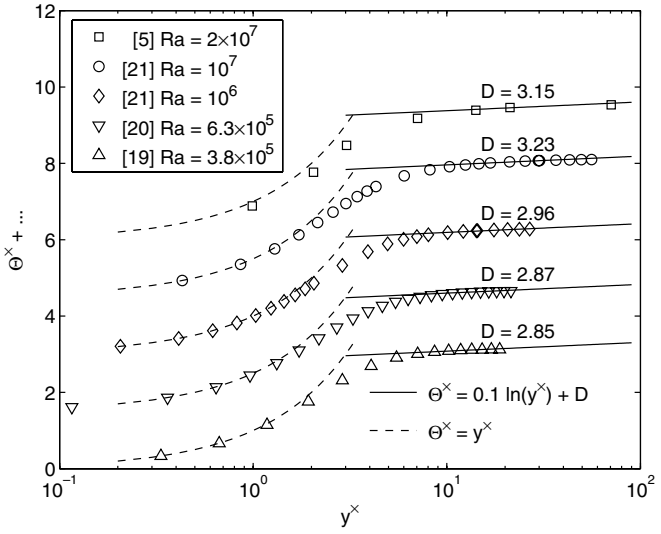

Fig. 2. Non-dimensionalized DNS temperature profiles for $Pr = 0.7$ ($0 \leqslant y \leqslant h/2$).

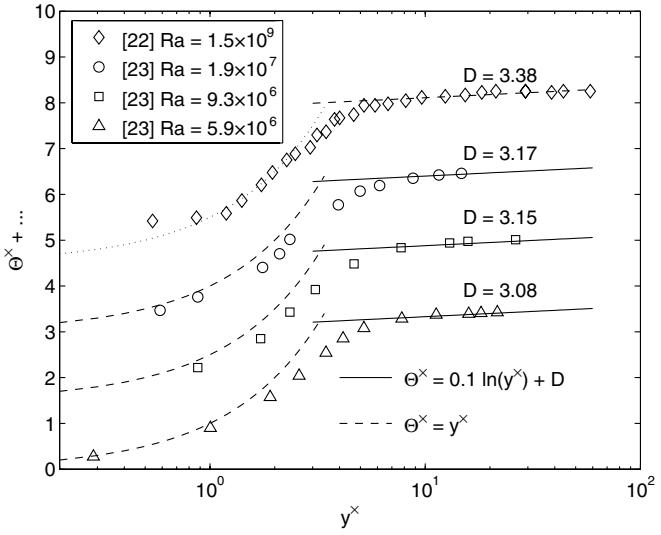

Fig. 3. Non-dimensionalized measured temperature profiles for $Pr = 5.4$.

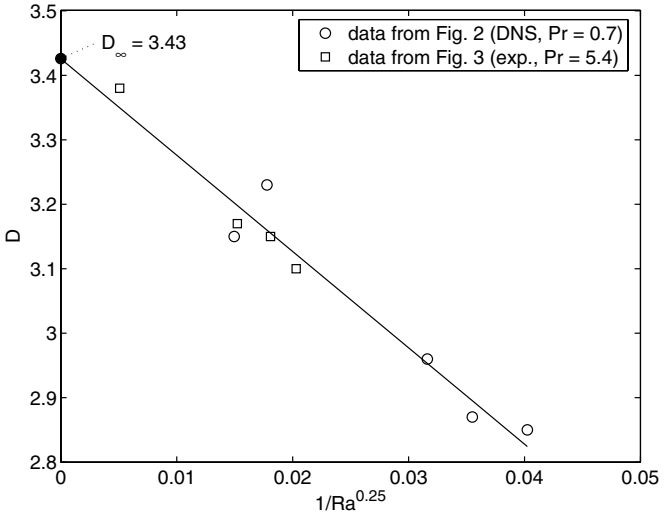

Fig. 4. Least square fit of D over $1/Ra^{0.25}$ for all data from Figs. 2 and 3.

This Rayleigh number dependence obviously is an effect of finite Rayleigh numbers, that are not yet large enough for the asymptotic representation ($Ra \to \infty$).

In order to extrapolate D for $Ra \to \infty$ from finite Rayleigh number data we correlate them by

$$D = -\frac{14.94}{Ra^{0.25}} + 3.43 \tag{15}$$

and thus get $D_\infty = 3.43$ for $Ra \to \infty$, see Fig. 4.

For high Rayleigh numbers ($Ra \to \infty$) the temperature profile according to our asymptotic approach therefore is

$$\Theta^\times = 0.1\cdot\ln(y^\times) + 3.43. \tag{16}$$

If any, there is no strong Prandtl number influence on the data shown by Fig. 4 which covers flows with $0.71 \leqslant Pr \leqslant 5.4$.

3. Nusselt–Rayleigh correlation

In the previous section the asymptotic form of the temperature profile was derived. Assuming the logarithmic profile to be approximately valid up to $y = h/2$ (cf. the DNS data in Fig. 2) our temperature profile can be transformed into a Nusselt–Rayleigh correlation, using $T(0) - T(h/2) = \Delta T/2$ in Eq. (12), i.e.

$$\frac{\Delta T/2}{T_c} = C\cdot\ln\left(\left|\frac{\partial T}{\partial y}\right|_w \cdot \frac{h/2}{T_c}\right) + D. \tag{17}$$

This can be rewritten as

$$Nu = \frac{Ra^{1/3}}{\left[\frac{C}{2}\ln\left(\frac{1}{16}\cdot Ra\cdot Nu\right) + 2\cdot D\right]^{4/3}} \tag{18}$$

with $C = 0.1$ and $D = -14.94\cdot Ra^{-0.25} + 3.43$, according to Eq. (15), or $D_\infty = 3.43$ as the asymptotic correlation for $Ra \to \infty$.

This Nusselt correlation is an implicit function and cannot be calculated directly. Table 3 in the Appendix shows

calculated values of the Nusselt number for different Rayleigh numbers as well as values from an approximation (22), see the Appendix, to this Nusselt correlation.

Correlation (18) can be used for $Pr \gtrsim 0.5$ since then the influence of the Prandtl number is negligible or at least within the measurement uncertainties, see for example Roche et al. [16] and Ahlers and Xu [24]. Verzicco and Camussi [25] in a numerical study showed that even for $Pr \gtrsim 0.35$ the Prandtl number influence can be neglected.

3.1. Comparison with experimental and numerical data

As mentioned in Section 1 already we only refer to experimental data that correctly take into account the conjugate heat transfer effects at the side walls. They are listed in Table 2 together with numerical data for which side wall conduction does not exist due to the imposed periodic boundary conditions.

In Fig. 5 $Nu(Ra)$ from measurements by Niemela and Sreenivasan [15] and DNS calculations by Kerr [5] are compared to Eq. (18) with D according to Eq. (15). Though Ra varies by ten orders of magnitude (10^5–10^{15}) the agreement is good.

In Fig. 6(a) and (b), all data of Table 2 are plotted as $Nu \cdot Ra^{-2/7}$ vs. Ra leading to a high resolution plot where deviations become more obvious. The exponent of $-2/7$ was chosen for "historical" reasons. Additionally, we show the correlations of Wu and Libchaber [4] in accordance with the 2/7th power law of Castaing et al. [2] and the 1/3rd power law of Goldstein and Tokuda [27] in accordance with Priestley [1]. To avoid confusion by too many data those for $Pr = 0.7$ are shown in Fig. 6(a) and those for $Pr > 0.7$ in Fig. 6(b).

In this high resolution plots it can be seen that the different data sets have no uniform behaviour, but show a moderate scatter. Nevertheless, the proposed Nusselt correlation (18) lies very well within the Nusselt data obviously closer to the data than the 1/3rd and 2/7th power laws according to [4] and [27], respectively.

It should be kept in mind, however, that our analysis was based on the assumption of plates of infinite extent ($\Gamma = \infty$; like in the DNS calculations) resulting in a heat transfer problem with no (time-averaged local) mean flow. However, since there are no experimental data with high aspect ratios ($\Gamma \to \infty$, i.e. with no mean flow) at high Rayleigh numbers we only can compare our Eq. (18) to data obtained in cells with $1/2 \leqslant \Gamma \leqslant 1$ where a mean flow exists. According to Ahlers and Xu [24] the influence of the aspect ratio is negligible for $1/2 \leqslant \Gamma \leqslant 1$. For $\Gamma = \infty$, however, deviations might occur that cannot be estimated properly. For example, Roche et al. [16] with $\Gamma = 1/2$ observed a bimodality for the Nusselt correlation (two different factors in front of the Rayleigh number in their power law) and explained it with two different flow situations that might develop in their cell. Small aspect ratios might be one reason for the inconsistency found in recent data sets and also might result in deviations between our Theory (18) and the data from Table 2.

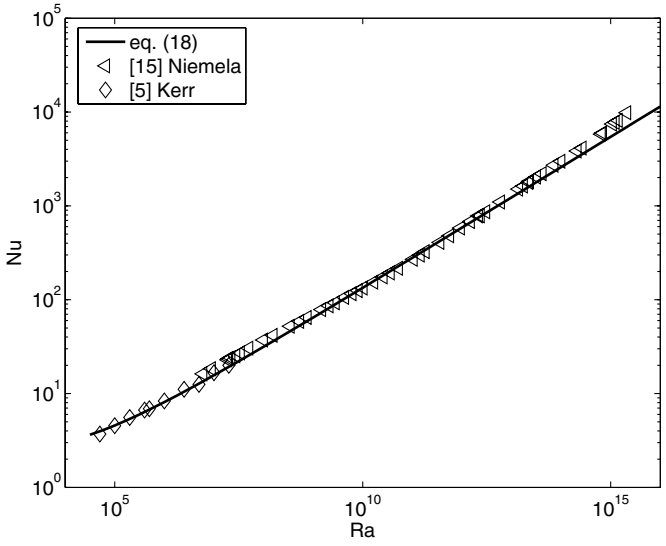

Fig. 5. $Nu(Ra)$ according to Niemela and Sreenivasan [15] and Kerr [5], both for $Pr = 0.71$, compared to Eq. (18).

3.2. Theory of Grossmann and Lohse

Along with the Theories of Priestley [1] and Castaing et al. [2] a third theory was established by Grossmann

Table 2
Data used in this study for comparison with the Nusselt–Rayleigh correlation (18)

Authors	Ra-range	Pr-range	Γ	Data
Niemela [9]	$10^6 < Ra < 10^{17}$	$Pr \approx 1$	1/2	–
Ashkenazi [12]	$10^9 < Ra < 5 \times 10^{15}$	$1 \leqslant Pr \leqslant 93$	1	–
Chavanne [13]	$10^5 < Ra < 2 \times 10^{14}$	$0.66 < Pr < 37$	1/2	√
Nikolaenko [14]	$3 \times 10^9 < Ra < 6 \times 10^{10}$	$Pr = 4.4$	1	–
Niemela [15]	$6 \times 10^6 < Ra < 2 \times 10^{15}$	$Pr \approx 1$	1	√
Roche [16]	$3 \times 10^8 < Ra < 10^{11}$	$0.7 < Pr < 21$	1/2	√
Ahlers [24]	$3 \times 10^7 < Ra < 10^{11}$	$4 < Pr < 34.1$	1/2 and 1	–
Kerr [5]^{DNS}	$5 \times 10^4 < Ra < 2 \times 10^7$	$Pr = 0.7$	∞	√
Hartlep [21]^{DNS}	$2 \times 10^3 < Ra < 10^7$	$Pr = 0.7$	∞	√
Verzicco [26]^{DNS}	$2 \times 10^6 < Ra < 2 \times 10^{11}$	$Pr = 0.7$	1/2	√

[...]^{DNS}: numerical studies (DNS); "√" in the last column: $Nu(Ra)$ is given explicitly in tabulated form; "–" in the last column: $Nu(Ra)$ is given in graphical form or as a power law.

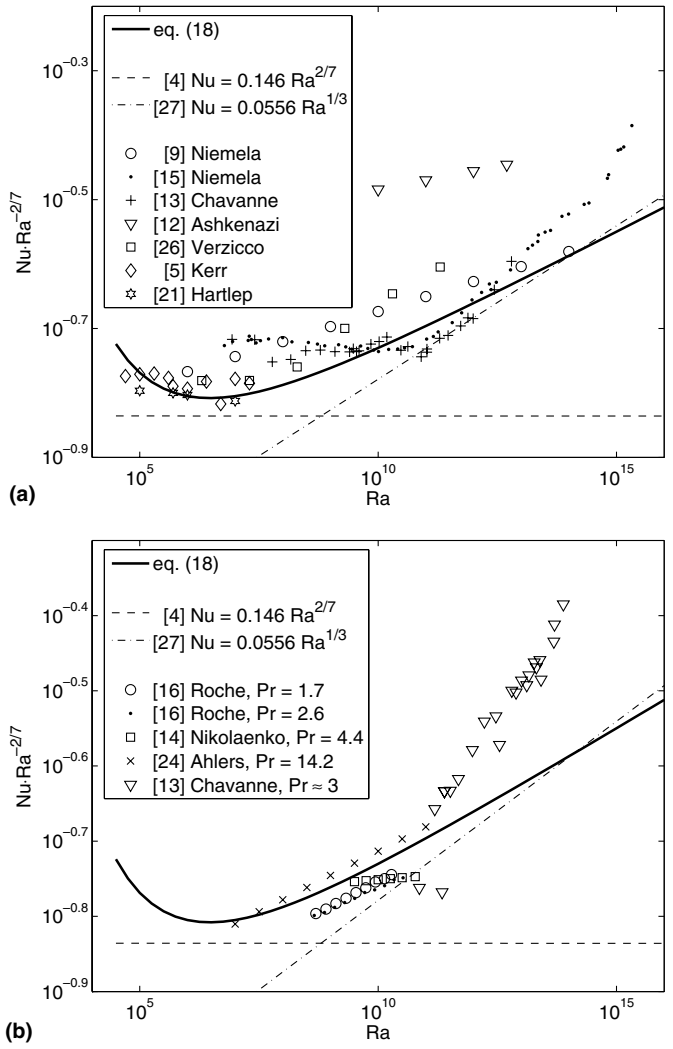

Fig. 6. (a) $NuRa^{-2/7}$ vs. Ra of experimental and DNS data for $Pr = 0.71$, compared to Eq. (18) and (b) $NuRa^{-2/7}$ vs. Ra of experimental data for $Pr > 0.71$ compared to Eq. (18).

and Lohse [6] which became widely accepted in the last few years. Their derivation of the Nusselt correlation is based on kinematic and thermal dissipation, that can be dominant either in the boundary layers or in the core region. To account for different cases, they introduced a Rayleigh Prandtl phase diagram and defined eight different regions with their own scalings. To obtain a Nusselt number correlation for a certain case, the Prandtl number and the range of Rayleigh numbers must be known in order to identify the appropriate regions in the phase diagram. The Nusselt number then is calculated as the superposition of two neighbouring regions. For more details how to use the Theory of Grossmann and Lohse [6] see also Xu et al. [7], who performed experiments with acetone ($Pr = 4.0$) and found good agreement with the Theory in [6].

In order to compare our Theory (18) and that of Grossmann and Lohse [6] to experimental data, we choose two different Prandtl numbers, $Pr \approx 0.7$ and $Pr \approx 3$. For $Pr \approx 0.7$, with the notation of the work of Grossmann and Lohse [6], the heat transfer is dominated by regime I_l and IV_u, leading to

$$Nu = \underbrace{0.27 \cdot Ra^{1/4} \cdot Pr^{-1/8}}_{I_l} + \underbrace{0.038 \cdot Ra^{1/3}}_{IV_u} \tag{19}$$

This correlation is plotted in Fig. 7(a) together with Eq. (18) against the data of Niemela and Sreenivasan [15] and Niemela et al. [9].

For $Pr \approx 0.7$ our Theory, Eq. (18), is in closer agreement to the experimental data than Eq. (19) according to the Theory by Grossmann and Lohse [6].

For $Pr \approx 3$, the regimes I_u and III_u in [6] are dominant, so that

$$Nu = \underbrace{0.33 \cdot Ra^{1/4} \cdot Pr^{-1/12}}_{I_u} + \underbrace{0.00343 \cdot Ra^{3/7} \cdot Pr^{-1/7}}_{III_u}. \tag{20}$$

This equation is shown in Fig. 7(b) together with our Eq. (18) and the data of Roche et al. [16] for $Pr = 2.6$ and Chavanne et al. [13] for $Pr \approx 3$.

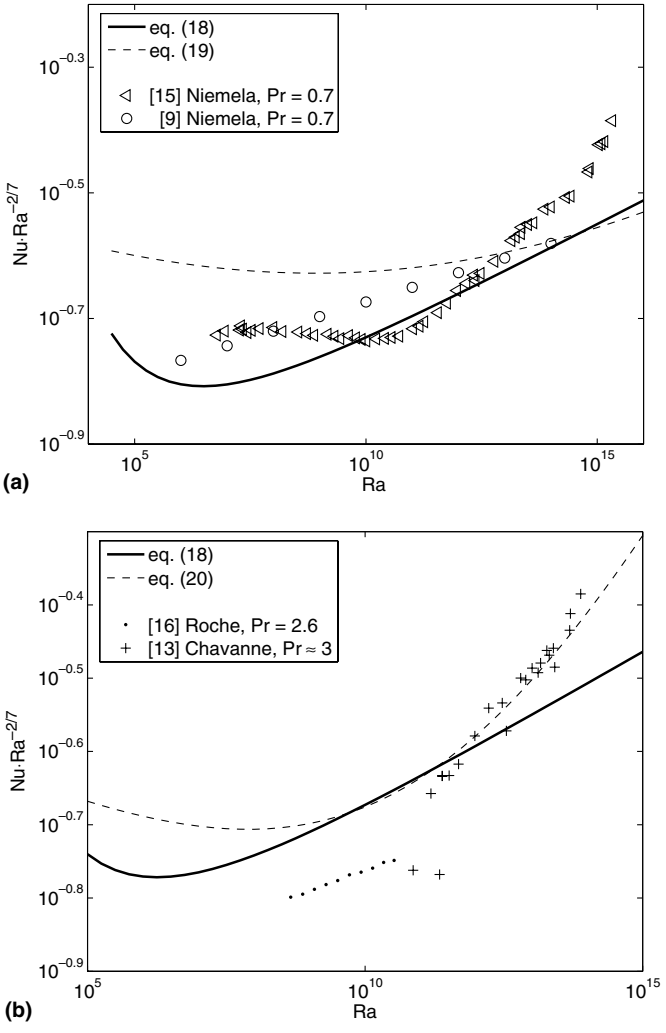

Fig. 7. Comparison of Eq. (18) and the Theory of [6] with experimental data at two Prandtl numbers: (a) $Pr = 0.7$ and (b) $Pr = 2.6$.

The data of Roche et al. [16] are badly represented by both theories, whereas Eq. (20) matches the data of Chavanne et al. [13] fairly well at high Rayleigh numbers.

At least for those (typical) cases shown here both theories perform equally well (or bad), though our Nusselt number correlation is much easier to handle.

3.3. Influence of surface roughness

In Fig. 6(a) and (b) a closer inspection reveals that the Nusselt number curves of Niemela and Sreenivasan [15] and Chavanne et al. [13] change their slope at very high Rayleigh numbers. Sometimes, this behaviour is believed to be connected to the *ultimate regime* proposed by Kraichnan [28]. An alternative explanation, however, would be the influence of the surface roughness, that will be estimated next.

The viscous sublayer expands from the wall up to $y^{\times} \approx 1.5$ since in this region the temperature profile is purely linear, see Figs. 2 and 3. If the surface roughness, k_s, lies within the viscous sublayer the surface is hydraulically smooth. If roughness elements stick out of the viscous sublayer, the temperature profile and therefore also the Nusselt number is effected by these elements.

Thus, the surface roughness is assumed to be of importance if

$$k_s^{\times} \equiv \frac{k_s}{T_c} \cdot \left|\frac{\partial T}{\partial y}\right|_w > 1.5 \quad \text{i.e.} \quad \frac{k_s}{h} > 1.5 \cdot (Ra \cdot Nu)^{-1/4}. \qquad (21)$$

The experiments of Niemela and Sreenivasan [15] and Chavanne et al. [13] both used copper top and bottom plates for which $k_s = 20\ \mu m$ can be assumed as a typical roughness height.[3] The cell heights were $h = 0.5$ m and $h = 0.2$ m, respectively. Now it can be estimated for which Rayleigh numbers roughness effects gain importance, i.e. for which Rayleigh numbers k_s/h is greater than $1.5 \cdot (Ra \cdot Nu)^{-1/4}$.

Fig. 8 shows a plot of $1.5 \cdot (Ra \cdot Nu)^{-1/4}$ vs. Ra with Eq. (18) for Nu together with the two roughness values. In [15] the non-dimensional roughness is $k_s/h = 4 \times 10^{-5}$, resulting in a Rayleigh number $Ra = 4.6 \times 10^{14}$ for which roughness effects should gain influence. The roughness in [13] is $k_s/h = 1.0 \times 10^{-4}$, leading to $Ra = 3 \times 10^{13}$. The inserted box in Fig. 8 shows the Nusselt data of Niemela and Sreenivasan [15] and Chavanne et al. [13]. In both cases, the slope of the Nusselt number changes for Rayleigh numbers just beyond the estimated values as indicated by the arrows in the inserted box. Given the uncertainties of k_s and of the width of the molecular sublayer ($y^{\times} \approx 1.5$), surface roughness effects might be a reasonable explanation, i.e. the change in the slope of the Nusselt number might not just be a Rayleigh number effect, as proposed by Kraichnan [28], but can also be explained by the disturbance of the molecular sublayer and is therefore a function of the Rayleigh number *and* height h of the cell.

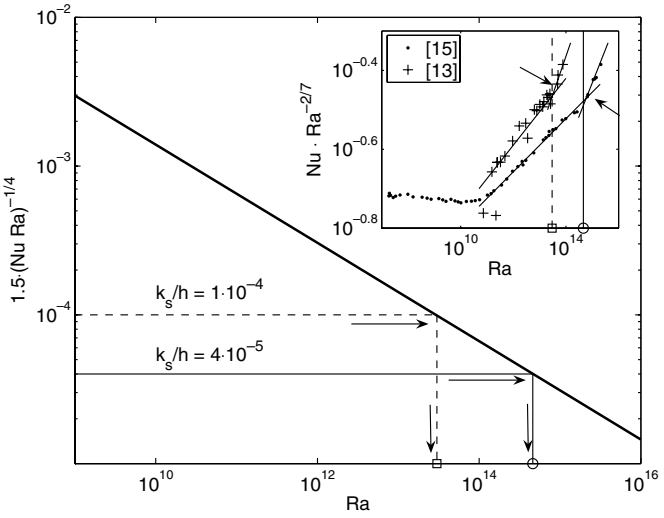

Fig. 8. $1.5 \cdot (NuRa)^{-1/4}$ vs. Ra, relevant for estimating the influence of the surface roughness. If the value of the non-dimensionlized roughness k_s/h is below the graph the roughness lies within the viscous sublayer and it can be neglected. For all Rayleigh numbers above the intersection, the Nusselt data should show a change in its behaviour. The inserted box shows the Rayleigh numbers for which we estimated deviations.

4. Conclusions

The structure of the temperature profile was analysed asymptotically and a logarithmic profile in the overlap layer was found. According to available temperature data for large but finite Rayleigh numbers, the logarithmic profiles depend on the Rayleigh number. After an extrapolation for $Ra \to \infty$, however, the asymptotic profile emerges. Nevertheless, it would be highly desirable to have measured or simulated temperature profiles for $Ra > 10^{10}$ with special attention paid to the temperature wall gradient, since this is the crucial parameter for the present analysis.

From the temperature profile a Nusselt number correlation can be deduced and compared to experimental and numerical data. This correlation covers existing data for $10^5 \leqslant Ra \leqslant 10^{15}$ better than the 1/3- and 2/7-power laws (see Priestley [1] and Castaing et al. [2]). Also, for $Pr > 0.5$, it is an alternative to the Theory of Grossmann and Lohse [6].

Additionally, we analysed surface roughness effects showing that once the roughness elements exceed the viscous sublayer deviations in the Nusselt number data occur in certain published experiments.

Appendix A

The Nusselt number correlation (18) is an implicit function and therefore Nu cannot be calculated directly. Though the correlation is easy to solve by iterations an approximation might be convenient.

[3] Schlichting and Gersten [29] give a equivalent sand roughness $k_{s\,eq} < 30\ \mu m$ for copper. To stay in this range we chose $k_s = k_{s\,eq} = 20\ \mu m$.

Table 3
Comparison of Nusselt numbers calculated with Eq. (18) and with the explicit approximation (22)

Ra	Nu, Eq. (18)	Nu_{appr}, Eq. (22)	r in %
10^5	4.566	4.569	0.07
10^6	8.123	8.116	−0.09
10^7	15.689	15.668	−0.13
10^8	31.526	31.483	−0.14
10^9	64.668	64.587	−0.13
10^{10}	134.135	133.992	−0.11
10^{11}	279.957	279.721	−0.08
10^{12}	586.404	586.048	−0.06
10^{13}	1230.938	1230.493	−0.04
10^{14}	2587.421	2587.122	−0.01
10^{15}	5443.761	5444.465	0.01

Here, r is the relative error in %, i.e. $(Nu_{\mathrm{appr}} - Nu)/Nu$.

For that purpose we replace Nu in the logarithmic term of Eq. (18) by the approximation $Nu = 0.078 \cdot Ra^{0.323}$ which holds for $Ra \to \infty$, and thus get

$$Nu = \frac{Ra^{1/3}}{\left[\frac{C}{2}\ln\left(\frac{0.078}{16}\cdot Ra^{1.323}\right) + 2\cdot D\right]^{4/3}} \tag{22}$$

$$C = 0.1 \tag{23}$$

$$D = -\frac{14.94}{Ra^{0.25}} + 3.43 \tag{24}$$

Table 3 gives some values of the Nusselt number calculated with the implicit Eq. (18), the explicit approximation (22) and the relative error r in %. Since the error always is less than ±0.2% the explicit formula is a useful approximation that is easier to handle.

References

[1] C.H.B. Priestley, Convection from a large horizontal surface, Austral. J. Phys. 7 (1954) 176–201.
[2] B. Castaing, G. Gunaratne, F. Heslot, L. Kadanoff, A. Libchaber, S. Thomae, X. Wu, S. Zaleski, G. Zanetti, Scaling of hard thermal turbulence in Rayleigh–Bénard convection, J. Fluid Mech. 204 (1989) 1–30.
[3] B.I. Shraiman, E.D. Siggia, Heat transport in high-Rayleigh-number convection, Phys. Rev. A 42 (1990) 3650–3653.
[4] X.-Z. Wu, A. Libchaber, Scaling relations in thermal turbulence: the aspect ratio dependence, Phys. Rev. A 45 (1992) 842–845.
[5] R. Kerr, Rayleigh number scaling in numerical convection, J. Fluid Mech. 310 (1996) 139–179.
[6] S. Grossmann, D. Lohse, Scaling in thermal convection: a unifying theory, J. Fluid Mech. 407 (2000) 27–56.
[7] X. Xu, K.M.S. Bajaj, G. Ahlers, Heat transport in turbulent Rayleigh–Bénard convection, Phys. Rev. Lett. 84 (2000) 4357.
[8] S. Grossmann, D. Lohse, Thermal convection for large Prandtl numbers, Phys. Rev. Lett. 86 (2001) 3316–3319.
[9] J.J. Niemela, L. Skrbek, K.R. Sreenivasan, R.J. Donnelly, Turbulent convection at very high Rayleigh numbers, Nature 404 (2000) 837–840.
[10] G. Ahlers, Effect of sidewall conductance on heat-transport measurements for turbulent Rayleigh–Bénard convection, Phys. Rev. E 63 (2001) 015303(R).
[11] R. Verzicco, Sidewall finite-conductivity effects in confined turbulent thermal convection, J. Fluid Mech. 473 (2002) 201–210.
[12] S. Ashkenazi, V. Steinberg, High Rayleigh number turbulent convection in a gas near the gas–liquid critical point, Phys. Rev. Lett. 83 (1999) 3641–3644.
[13] X. Chavanne, F. Chilla, B. Chabaud, B. Castaing, B. Hébral, Turbulent Rayleigh–Bénard convection in gaseous and liquid He, Phys. Fluids 13 (2001) 1300–1320.
[14] A. Nikolaenko, G. Ahlers, Nusselt number measurements for turbulent Rayleigh–Bénard convection, Phys. Rev. Lett. 91 (2003) 084501.
[15] J.J. Niemela, K.R. Sreenivasan, Confined turbulent convection, J. Fluid Mech. 481 (2003) 355–384.
[16] P.-E. Roche, B. Castaing, B. Chabaud, B. Hébral, Heat transfer in turbulent Rayleigh–Bénard convection below the ultimate regime, J. Low Temp. Phys. 134 (2004) 1011–1042.
[17] H. Schlichting, K. Gersten, Boundary-layer Theory, eighth ed., Springer, Berlin, 2003, pp. 517–523.
[18] M. Hölling, H. Herwig, Asymptotic analysis of the near wall region of turbulent natural convection flows, J. Fluid Mech. 541 (2005) 383–397.
[19] G. Grötzbach, Simulation of turbulent flow and heat transfer for selected problems of nuclear thermal-hydraulics, in: Proc. First Int. Conf. on Supercommuting in Nuclear Applications (SNA '90), Mito, Japan, March 12–16, 1990.
[20] M. Wörner, Direkte Simulation turbulenter Rayleigh–Benard Konvektion in flüssigem Natrium, Ph.D. Thesis, University of Karlsruhe, KfK 5228, 1994.
[21] T. Hartlep, Strukturbildung und Turbulenz. Eine numerische Studie zur turbulenten Rayleigh–Bénard Konvektion, Ph.D. Thesis, University of Göttingen, 2004.
[22] Y.-B. Du, P. Tong, Turbulent thermal convection in a cell with ordered rough boundaries, J. Fluid Mech. 407 (2000) 57–84.
[23] T.Y. Chu, R.J. Goldstein, Turbulent convection in a horizontal layer of water, Int. J. Heat Mass Transfer 60 (1973) 141–159.
[24] G. Ahlers, X. Xu, Prandtl-number dependence of heat transport in turbulent Rayleigh–Bénard convection, Phys. Rev. Lett 86 (2001) 3320.
[25] R. Verzicco, R. Camussi, Prandtl number effects in convective turbulence, J. Fluid Mech. 383 (1999) 55–73.
[26] R. Verzicco, R. Camussi, Numerical experiments on strongly turbulent thermal convection in a slender cylindrical cell, J. Fluid Mech. 477 (2003) 19–49.
[27] R.J. Goldstein, S. Tokuda, Heat transfer by thermal convection at high Rayleigh numbers, Int. J. Heat Mass Transfer 23 (1980) 738–740.
[28] R.H. Kraichnan, Turbulent thermal convection at arbitrary Prandtl number, Phys. Fluids 5 (1962) 1374–1389.
[29] H. Schlichting, K. Gersten, Boundary-layer Theory, eighth ed., Springer, Berlin, 2003, pp. 529–531.